

SynthIPD: assumption-lean synthetic individual patient data generation

Zixuan Zhao, Zexin Ren, Guannan Zhai and Feifang Hu
Department of Statistics, The George Washington University
Will Ma, En Xie
HopeAI, Inc.
Qian Shi
Mayo Clinic

September 23, 2025

Abstract

Individual patient data (IPD) are essential for statistical inference in clinical research. However, privacy concerns, high data-sharing costs, and restrictive access often make IPD unavailable. Conventional synthetic data generation usually relies on black box models such as generative adversarial networks. These methods, however, requires a large piece of IPD for model training, may be ungeneralizable and lacks interpretability. This paper introduces an *assumption-lean*, three-step methodology for generating synthetic IPD with survival endpoints only based on published clinical trial articles. The method mainly leverages Kaplan-Meier (KM) curves with at-risk/censoring information and subgroup-level summary statistics. It digitizes the KM curve using Scalable Vector Graphics (SVG) beyond pixel accuracy and then generates synthetic covariates based on the statistics. We illustrate the method's potential through 2 detailed case studies and simulation studies. The method offers important implications, enabling high-fidelity IPD generation to support evidence-based medical decisions.

Keywords: Synthetic data generation, True IPD free, Scalable Vector Graphics, survival analysis, Kaplan-Meier curve

1 Introduction

1.1 Motivation and key applications

In clinical trial design, covariate-adaptive randomization can ensure balanced confounders across treatment groups [22, 17, 32, 18] and valid statistical inference [25, 43, 26, 24], while Bayesian adaptive trial designs learn about treatment effects efficiently by using accumulating outcome data to update beliefs and aims to reduce the required sample size to reach a target power [35, 46, 3]. In many rare-disease indications, or in highly stratified settings, even these efficiency improvements are not enough: the eligible population is simply too small to support a conventional randomization within a reasonable time frame. This drives the need for research in reliable synthetic data generation method. With the help of synthetic IPD, it may be possible to establish synthetic control methods that largely reduce required sample sizes. Moreover, when planners have access only to aggregate summaries, sample-size estimates can be biased and design choices can be sub-optimal. A method that can faithfully reconstruct IPD would therefore provide reasonable estimates and enhance trial designs.

This work introduces SynthIPD, a novel three-step approach leveraging only published clinical trial results to accurately generate synthetic IPD. First, the coordinates of each event are first digitized with high accuracy from published KM plots utilizing properties of Scalable Vector Graphics (SVG). Secondly, covariate data are generated and matched via a constrained optimization approach. Finally, survival and covariate data are combined, producing a final synthetic dataset.

SynthIPD enables numerous applications: (i) Gain new statistical insights: The synthetic IPD closely follows the distribution of the true IPD and can offer new statistical in-

sights that are not originally reported in the paper [39]. (ii) Establish control benchmarks: By pooling synthetic IPD from the control arms of historical trials, investigators can establish an accurate endpoint estimation for the control arm and further guide subsequent sample size calculation [44, 21, 48], which is crucial for clinical trial design. (iii) Construct synthetic control arms: As mentioned in 2023 FDA guideline [41], clinical trial IPD have advantages over other sources. SynthIPD, creating synthetic clinical trial data, offers a potential way to replace or augment control arms that can boost statistical efficiency while preserving robustness of subsequent statistical analyses. (iv) Validate aggregated analyses: Pooled analyses using IPD can validate and improve the reliability of conventional meta-analyses [38, 34], which may suffer from bias if some critical assumptions are not satisfied. (v) Serve as the training set for other synthetic data methods: SynthIPD does not require any training, and hence can serve as the training set (or ‘pseudo IPD’) for other models, e.g., GAN models, when the IPD are unavailable, see Subsection 4.3.

The credibility of our proposed algorithm enables reliable analysis. We have readily verified its applicability by conducting a surrogacy analysis between minimal residual disease and PFS [33]. Furthermore, the effectiveness of our method is demonstrated through two case studies, covering (i), (ii), (iv). The first case involves reconstructing IPD from the N9741 colorectal cancer trial [12], showing remarkable similarity with the actual trial data. In the second case study, synthetic IPD for six different Multiple Myeloma (MM) trials are generated ($n = 4061$) and a pooled analysis is conducted to validate the clinical benefit of Daratumumab in high-risk cytogenetic patients. The results obtained using synthetic IPD closely align with conventional random-effect meta-analysis findings. Benchmark progression free survival times based on these trials for different cytogenetic risk subgroups treated by Daratumumab are also established using our method.

The robustness of our method is further validated through extensive simulation studies. The difference between true and SynthIPD are measured by several metrics that measure distributional differences. Results show that the generated synthetic IPD possesses similar distribution with the simulated, true IPD.

1.2 Existing approaches

Several strategies have been developed with the aim of generating synthetic data sets. One of the most commonly seen approach is to synthesize entirely new datasets based on generative models, e.g., [2, 15, 29]. Given the large number of similar methods, we refer readers to [1] for a detailed reading therein. Yet, synthetic datasets created by these method typically require a reasonably large piece of true IPD to train. Also, they may lack generalizability because the training data may be heterogeneous.

Other approaches focus on reconstructing survival times from published KM plots, either manually or with the assistance of large language models (LLMs) [14, 23, 45]. These methods have relatively low accuracy and cannot incorporate covariate structures and subgroup-specific effects, limiting their utility in practice. Some techniques attempt to impute missing covariates by imposing distributional assumptions or by leveraging externally available population summaries [31, 13], but such imputations can introduce bias if the underlying assumptions are violated.

1.3 Our contributions

Our contribution is multi-folds. First, almost all model-based synthetic data generation techniques requires IPD for training, and relies heavily on the training data source and its generalizability. Our method, on the other hand, does not require any IPD or extra

information other than what are provided in published clinical trial articles. Second, the core step of our method is an interpretable optimization procedure. Third, our method generates IPD with corresponding covariate information, which allows statistical analyses on subgroups representing a significant advance for clinical research, facilitating detailed analyses that were previously infeasible without direct IPD access.

The remainder of the paper is structured as follows: Section 2 details preliminary concepts, defines loss functions for accuracy assessment, and elaborates on the proposed three-step algorithm. Section 3 discusses two detailed real-world applications. Section 4 conducts simulation studies validating method performance and presents a toy comparison study with survivalGAN [29], a recently proposed GAN model for generating survival data. Section 5 concludes future directions.

2 Proposed method

2.1 Preliminaries

Consider a clinical trial study of n patients with survival outcome. For the i th patient, denote the observed survival time $U_i = \min(T_i, C_i)$, where T_i is the time to disease progression or death, C_i is the administrative censoring time and $\Delta_i = \mathbb{1}\{T_i \leq C_i\}$ is the censoring status. Let A_i be the treatment assignment, that is, $A_i = 1$ if active treatment and $A_i = 0$ if control. For simplicity, set X_i to be a univariate categorical covariate, taking values in $\{0, \dots, K\}$. In fact, covariates can be multivariate categorical as long as the total number of strata it produces is finite and can be, without loss of generality, transformed into a univariate X_i . The (true) IPD from a trial with survival endpoint is defined as the collection $D_n := \{U_i, \Delta_i, A_i, X_i\}_{i=1}^n$ with finite sample realization $d_n = \{u_i, \delta_i, a_i, x_i\}_{i=1}^n$.

The goal is to generate a synthetic copy

$$\tilde{d}_n := \left\{ \tilde{d}_n^{(-x)}, \{\tilde{x}_i\}_{i=1}^n \right\} = \{\tilde{u}_i, \tilde{\delta}_i, \tilde{a}_i, \tilde{x}_i\}_{i=1}^n$$

with similar statistical properties as d_n .

For each treatment arm $a \in \{0, 1\}$ and subgroup $x \in \{0, \dots, K\}$, let n_x (resp. $n_{x,a}$) be the number of patients in subgroup x (resp. subgroup x , treatment a). Denote by

$$S_a(t) := P(T \geq t \mid A = a), \quad S_{x,a}(t) := P(T \geq t \mid A = a, X = x)$$

the survival functions stratified by treatment or treatment and covariate. The hazard function and conditional hazard function can be expressed as

$$\lambda_a(t) = \lambda_0(t) \exp(\theta a), \quad \lambda_{x,a}(t) = \lambda_x(t) \exp(\theta_x a)$$

respectively, where $\lambda_0(t), \lambda_x(t)$ are the baseline hazard functions, θ, θ_x are the treatment effects. Commonly used statistics describing the distribution of T within subgroup $A = a, X = x$ includes the median survival time and conditional hazard ratio

$$m_{x,a} := \inf\{t : S_{x,a}(t) \leq 0.5\}, \quad \text{HR}_x := \exp(\theta_x).$$

Given data d_n , finite-sample estimates for above statistics and their 95% confidence intervals (95% CI) can be obtained easily by using standard survival analysis packages, e.g., R package ‘survival’. The finite-sample estimates $\hat{m}_{x,a}, \hat{\text{HR}}_x$ are essentially functions of the form

$$\hat{g}_x : d_{n,x} \mapsto \hat{g}_x(d_{n,x}) \in \mathbb{R}, \quad \hat{g}_{x,a} : d_{n,x,a} \mapsto \hat{g}_{x,a}(d_{n,x,a}) \in \mathbb{R}$$

where d_n is the IPD, $d_{n,x}$ (resp. $d_{n,x,a}$) is the IPD in subgroup $X = x$ (resp. in subgroup $X = x, A = a$). Further, for any type of estimate, we define the collection

$$\mathcal{J}_{\hat{g}} := \{\hat{g}, \text{lower 95\% CI of } \hat{g}, \text{upper 95\% CI of } \hat{g}\}$$

and adopt relative absolute error (RAE) that penalize worst-case discrepancies across all reported summary statistics:

$$\mathcal{L}_m(\tilde{d}_n \mid d_n) := \max_{\hat{g}_{x,a} \in \mathcal{J}_{\hat{m}_{x,a}}} \left| \frac{\hat{g}_{x,a}(d_{n,x,a}) - \hat{g}_{x,a}(\tilde{d}_{n,x,a})}{\hat{g}_{x,a}(d_{n,x,a})} \right|. \quad (1)$$

$$\mathcal{L}_{\text{HR}}(\tilde{d}_n \mid d_n) := \max_{\hat{g}_x \in \mathcal{J}_{\widehat{\text{HR}}_x}} \left| \frac{\hat{g}_x(d_{n,x}) - \hat{g}_x(\tilde{d}_{n,x})}{\hat{g}_x(d_{n,x})} \right|. \quad (2)$$

For simplicity, we use $\mathcal{L}_m, \mathcal{L}_{\text{HR}}$ if no confusion is introduced. In the best case, with $\tilde{d}_n = d_n$, the losses will be exactly 0's. These two losses will be a crucial quantity in our method and will be used as one of the similarity measures between two IPDs.

2.2 A three-step algorithm

Suppose a clinical trial study with two treatment is of interest but no IPD is available. Instead, the following are published in, possibly, a list of peer-reviewed clinical trial articles: a KM survival curve for all randomized patients in treatment (resp. control) denoted by \mathcal{G}_1 (resp. \mathcal{G}_0) in *Scalable Vector Graphics(SVG)* format along with a shared time grid $\mathcal{T} := \{t_0, \dots, t_\ell\}$ and an at risk number count $\mathcal{N}_1 = \{N_{1,t_0}, \dots, N_{1,t_\ell}\}$ (resp. $\mathcal{N}_0 = \{N_{0,t_0}, \dots, N_{0,t_\ell}\}$); the summary statistics within subgroups $\hat{\mathcal{J}}_{\hat{m}_{x,a}}, \hat{\mathcal{J}}_{\widehat{\text{HR}}_x}$.

The set of information $\{\mathcal{G}_a, \mathcal{N}_a, \mathcal{T} : a \in \{0, 1\}\}$ is crucial for the generation of survival IPD without covariate information. Then, $\hat{\mathcal{J}}_{\hat{m}_{x,a}}, \hat{\mathcal{J}}_{\widehat{\text{HR}}_x}$ are used to generate synthetic covariates. The SynthIPD method can be formalized into a three-step procedure:

- (1) a digitization step (DIGITIZE($\mathcal{G}_a, \mathcal{N}_a, \mathcal{T} : a \in \{0, 1\}$)) producing $\tilde{d}_n^{(-x)}$.
- (2) a covariates-generation step (cov-Gen($\tilde{d}_n^{(-x)}, \hat{\mathcal{J}}_{\hat{m}_{x,a}}, \hat{\mathcal{J}}_{\widehat{\text{HR}}_x}; R, H, a, b, f$)) producing $\{\tilde{x}_i\}_{i=1}^n$,

where R, H, a, b, f are hyper-parameters.

- (3) a combination step which combines the data in (1),(2) into \tilde{d}_n . The third step is straight forward and requires no further explanation.

Figure 1: The workflow of SynthIPD.

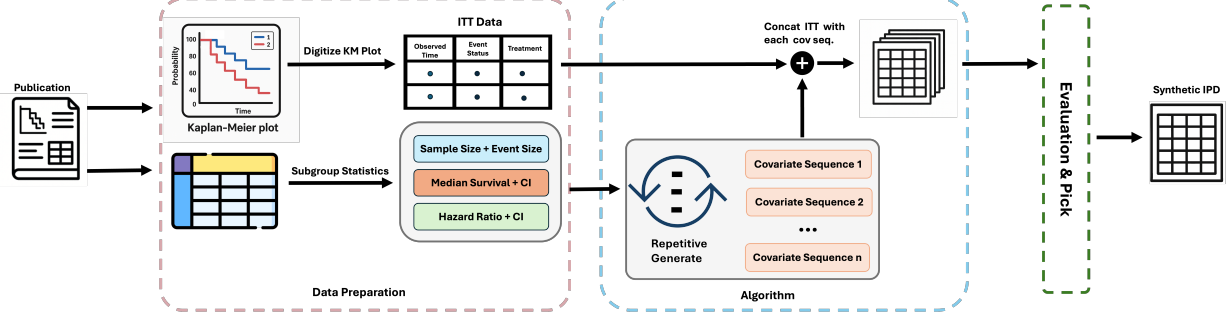


Table 1: Overview of inputs and outputs for each step.

| Step | Input | Hyper-parameters | Output |
|--------------|--|------------------|---------------------------|
| (1) DIGITIZE | $\mathcal{G}_1, \mathcal{G}_0, \mathcal{N}_1, \mathcal{N}_0, \mathcal{T}$ | None | $\tilde{d}_n^{(-x)}$ |
| (2) cov-Gen | $\tilde{d}_n^{(-x)}, \hat{\mathcal{J}}_{\hat{m}_{x,a}}, \hat{\mathcal{J}}_{\widehat{\text{HR}}_x}$ | R, H, a, b, f | $\{\tilde{x}_i\}_{i=1}^n$ |
| (3) combine | $\tilde{d}_n^{(-x)}, \{\tilde{x}_i\}_{i=1}^n$ | None | \tilde{d}_n |

To clarify, Table 1 is presented with inputs and outputs for each step and a flow chart of our method is shown in Figure 1. The implementation of the proposed algorithm requires several practical requirements, which is not stringent and can be satisfied by the publications in most high quality clinical journal publications. A real illustrative example of $\mathcal{G}_a, \mathcal{N}_a, \mathcal{T}, a \in \{0, 1\}, \hat{\mathcal{J}}_{\hat{m}_{x,a}}, \hat{\mathcal{J}}_{\widehat{\text{HR}}_x}$ is presented in Example 1. Although the requirements may appear extensive, it is highly likely that we can locate this information in the follow-up report. For example, for the ARROW study [7, Figure 1,2] contains subgroup information for age, CrCL, prior lines of therapy and refractory to bortezomib subgroups, which are not initially reported in the primary publication [28].

Remark. *For simplicity, we assume all aforementioned information are readily available to the researcher. When the SVG requirement is not satisfied, the digitization step can also be done by web plot digitizer (e.g., <https://automeris.io>) and IPDfromKM package [23] or*

KM-GPT [45], sacrificing modest degree of precision, see 4.1.

2.2.1 DIGITIZE

The coordinates of the KM plot (corresponding to *unique* observed times and survival probabilities $\{\tilde{u}_i, \hat{S}(\tilde{u}_i)\}_{i=1}^M, M \leq n$) can be extracted from the SVG using software tools like FIGMA. Additionally, $\tilde{a}_i, \tilde{\delta}_i, i \in [M]$ are available from the graph directly. If $M = n$, then all extracted coordinates are unique and the digitization is readily done. Conversely, $M < n$ indicates multiple events/censorings occurring at some time points. DIGITIZE($(\mathcal{G}_a, \mathcal{N}_a, \mathcal{T}) : a \in \{0, 1\}$), which is described as follows, is used to estimate the repeated events/censorings.

For each KM line $\mathcal{G}_a, a \in \{0, 1\}$, and index $\iota \in \{0, \dots, \ell\}$, within the time grid $[t_\iota, t_{\iota+1})$,

1. If numbers of censorings are not reported, estimate total number of events within

$[t_\iota, t_{\iota+1})$ by

$$\hat{e}_{a,\iota+1} = N_{a,t_\iota} \left(1 - \frac{\hat{S}_a(t_{\iota+1})}{\hat{S}_a(t_\iota)} \right),$$

where the subscript a is used to denote treatment arm and N_{a,t_ι} is the at risk number at time t_ι in arm a . Then, estimate the total number of censorings by $\hat{c}_{a,\iota+1} = N_{a,t_\iota} - \hat{e}_{a,\iota+1}$.

2. Estimate the average drop in survival probability for one single event between $[t_\iota, t_{\iota+1})$

by

$$p_{a,\iota+1} = \frac{\hat{S}_a(t_\iota) - \hat{S}_a(t_{\iota+1})}{\hat{e}_{a,\iota+1}}.$$

For a unique event time $t \in [t_\iota, t_{\iota+1})$, calculate the total drop by $\hat{S}_a(t) - \hat{S}_a(t^*)$, where t^* is the closest unique observed time point after t . Then, estimate the number of events at t by

$$\hat{E}_{a,t} = \frac{\hat{S}_a(t) - \hat{S}_a(t^*)}{p_{a,\iota+1}}.$$

3. Assign $\hat{E}_{a,t}$ events to time t . Distribute $\hat{C}_{a,t'}$ censorings uniformly to the unique censoring time points $t' \in [t_\iota, t_{\iota+1})$ so that $\sum_{t'} \text{unique censoring } \hat{C}_{a,t'} = \hat{c}_{a,\iota+1}$. Adjust $\hat{E}_{a,t}, \hat{c}_{a,\iota+1}$ so that $\sum_t \text{unique failure } \hat{E}_{a,t} + \hat{c}_{a,\iota+1} = N_{a,t_{\iota+1}}$

Repeat Step 1. – 3. until all time grids in \mathcal{T} are traversed. As an example, a real trial suitable for digitization is provided.

Example 1 (Candor study [42]). *The CANDOR study compares the use of carfilzomib, daratumumab, and dexamethasone (KdD) versus carfilzomib and dexamethasone (Kd) in relapsed or refractory Multiple Myeloma patients. The primary efficacy result is PFS. The reported KM plot for PFS is provided in Figure 2 and the subgroup summary statistics are reported in Figure 3.*

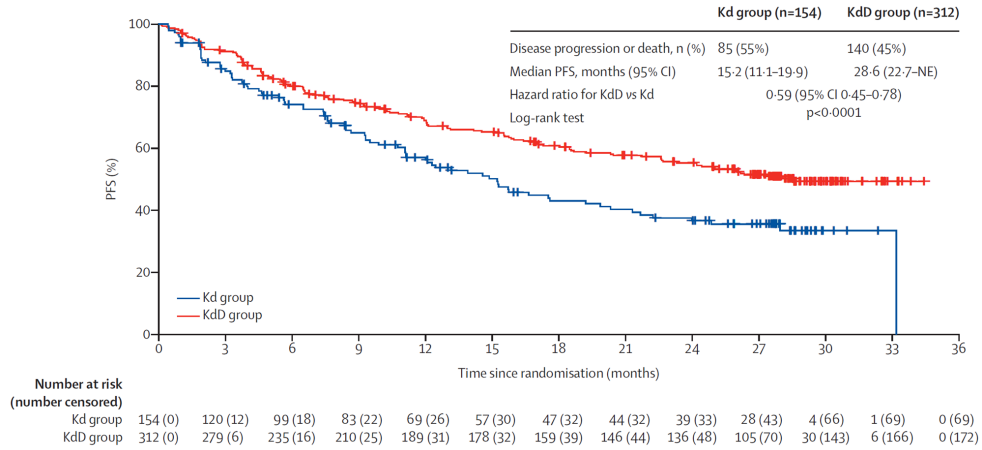


Figure 2: Reported $\mathcal{G}_1, \mathcal{G}_0$ for CANDOR study in the primary publication [42, Figure 2] with $\mathcal{T} = \{0, 3, 6, \dots, 36\}$, $\mathcal{N}_1 = \{312, 279, \dots, 0\}$, $\mathcal{N}_0 = \{154, 120, \dots, 0\}$, $\hat{c}_{1,1} = 0, \hat{c}_{1,2} = 6, \hat{c}_{0,1} = 0, \hat{c}_{0,2} = 12$, etc.

The digitization step above is similar but different from the IPDfromKM method [23] in the literature, where they use Tukey’s fence [40] to detect outliers due to manual extraction of coordinates. Since the points extracted via SVG are coordinate-wise accurate, the outlier

| | KdD group (n=312) | | Kd group (n=154) | | | Hazard ratio for KdD vs Kd (95% CI) |
|-------------------------|-------------------------|--------------------------------|-------------------------|--------------------------------|--|--|
| | Events/ participants | Median PFS, months (95% CI) | Events/ participants | Median PFS, months (95% CI) | | |
| ISS stage at screening* | | | | | | |
| I or II | 101/252 | NE (27.4-NE) | 68/127 | 15.8 (12.3-24.0) | | 0.60 (0.44-0.81) |
| III | 39/60 | 13.0 (8.8-18.5) | 17/27 | 7.4 (1.9-15.3) | | 0.57 (0.32-1.03) |
| Age at baseline, years | | | | | | |
| ≤65 | 79/178 | 28.6 (22.6-NE) | 50/80 | 14.9 (9.5-17.6) | | 0.51 (0.35-0.73) |
| >65 | 61/134 | 25.9 (18.6-NE) | 35/74 | 15.3 (9.3-NE) | | 0.73 (0.48-1.12) |

Figure 3: Reported summary statistics $\hat{\mathcal{J}}_{\hat{m}_{x,a}}, \hat{\mathcal{J}}_{\widehat{\text{HR}}_x}$ in the primary publication [42, Figure 3]. As an example, consider $X \in \{\text{Age} \leq 65, \text{Age} > 65\} := \{0, 1\}$, then $n_{0,0} = 80$, $\hat{m}_{0,0} = 14.9$, $\widehat{\text{HR}}_0 = 0.51$.

detection is unnecessary. Additionally, since SVG-based tools can provide us with the number of unique event and unique censoring times m , the new procedure is expected to mimic the KM behavior more accurately than IPDfromKM. See Subsection 4.1 for further comparison.

2.2.2 cov-Gen

After finishing the digitization step, we obtain $\tilde{d}_n^{(-x)}$. The generation step aims to create a vector $\{\tilde{x}_i\}_{i=1}^n$ such that the statistical properties of the combined synthetic sample \tilde{d}_n will be similar to that of d_n .

Our first try is to generate the covariate vector repeatedly from $\text{Multinomial}(n, (n_0/n, \dots, n_K/n))$ distribution and select the best covariate vector possible according to some criteria, e.g., the vector with minimal $\mathcal{L}_m, \mathcal{L}_{\text{HR}}$. This approach is natural because n_x/n is guaranteed to approximate the distribution of X well for large sample. However, it has two major drawbacks: First, it is computationally intensive to traverse all possible vectors $\{0, \dots, K\}^n$ as n, K increases. Secondly, it does not make use of the information $n_{x,a}$ provided in the subgroup analysis table. To improve upon these two drawbacks, we propose the cov-Gen($\tilde{d}_n^{(-x)}, \hat{\mathcal{J}}_{\hat{m}_{x,a}}, \hat{\mathcal{J}}_{\widehat{\text{HR}}_x}; R, H, a, b, f$) Algorithm 1.

Algorithm 1 cov-Gen($\tilde{d}_n^{(-x)}, \hat{\mathcal{J}}_{\hat{m}_{x,a}}, \hat{\mathcal{J}}_{\widehat{\text{HR}_x}}; R, H, a, b, f$)

(1) Randomly generate $\tilde{x}_i \in \{0, \dots, K\}^n$ such that $\tilde{n}_{x,a} = n_{x,a}$ for every $x \in [K], a \in \{0, 1\}$, let $\tilde{d}_n = \{\tilde{u}_i, \tilde{\delta}_i, \tilde{a}_i, \tilde{x}_i\}_{i=1}^n$. Calculate the corresponding statistics $\hat{\mathcal{J}}_{\hat{m}_{x,a}}, \hat{\mathcal{J}}_{\widehat{\text{HR}_x}}$.

(2) Calculate the losses $\mathcal{L}_m(\tilde{d}_n | d_n), \mathcal{L}_{\text{HR}}(\tilde{d}_n | d_n)$ via Equations (1),(2).

for $r \in [R]$ **do**

 Generate α from $\text{Unif}(a, b)$.

 Randomly switch $\alpha\%$ ($\alpha \in (a, b)$) of the entries in \tilde{x}_i , denote by $\tilde{x}_i^{(r)}$. Let $\tilde{d}_n^{(r)} = \{\tilde{u}_i, \tilde{\delta}_i, \tilde{a}_i, \tilde{x}_i^{(r)}\}_{i=1}^n$.

 Calculate the sets of statistics $\hat{\mathcal{J}}_{\hat{m}_{x,a}}, \hat{\mathcal{J}}_{\widehat{\text{HR}_x}}$.

if $\mathcal{L}_m(\tilde{d}_n^{(r)} | d_n) < \mathcal{L}_m(\tilde{d}_n | d_n)$ and $\mathcal{L}_{\text{HR}}(\tilde{d}_n^{(r)} | d_n) < H$ **then**

 Accept $\tilde{d}_n = \tilde{d}_n^{(r)}, \tilde{x}_i = \tilde{x}_i^{(r)}, \gamma = \gamma + 1$, continue to the next repetition.

else if $\mathcal{L}_m(\tilde{d}_n^{(r)} | d_n) = \mathcal{L}_m(\tilde{d}_n | d_n)$ and $\mathcal{L}_{\text{HR}}(\tilde{d}_n^{(r)} | d_n) < \mathcal{L}_{\text{HR}}(\tilde{d}_n | d_n)$ **then**

 Accept $\tilde{d}_n = \tilde{d}_n^{(r)}, \tilde{x}_i = \tilde{x}_i^{(r)}, \gamma = \gamma + 1$, continue to the next repetition.

else if $\mathcal{L}_m(\tilde{d}_n^{(r)} | d_n) > \mathcal{L}_m(\tilde{d}_n | d_n)$ and $\mathcal{L}_{\text{HR}}(\tilde{d}_n^{(r)} | d_n) \leq H$ **then**

 Accept $\tilde{d}_n = \tilde{d}_n^{(r)}, \tilde{x}_i = \tilde{x}_i^{(r)}$ with probability $f(\Delta^{(r)}, \gamma)$, where $\Delta^{(r)} = \mathcal{L}_m(\tilde{d}_n^{(r)} | d_n) - \mathcal{L}_m(\tilde{d}_n | d_n)$ and f satisfies Assumption 1.

else if $\mathcal{L}_{\text{HR}}(\tilde{d}_n^{(r)} | d_n) \geq H$ **then**

 Continue to the next repetition.

end if

end for

Report \tilde{d}_n as the final synthetic data.

Algorithm 1 requires information from digitization, iteratively updates subgroup vectors that can minimize median- and HR-based losses (1),(2) with hyper-parameters (R, H, a, b, f) .

In the algorithm, γ records the number of times \mathcal{L}_m decreases and $\gamma \rightarrow \infty$ as $r \rightarrow \infty$. The

hyper-parameter R controls the total number of iterations, H is a user-specified upper bound for HR loss, a, b decide the proportion of indices to swap for each step. The following assumption is needed for f .

Assumption 1. *The real-valued function $f : (0, \infty) \rightarrow (0, 1)$ satisfies $\lim_{\Delta^{(r)} \rightarrow \infty} f(\Delta^{(r)}, \cdot) \rightarrow 0$, $\lim_{\gamma \rightarrow \infty} f(\cdot, \gamma) \rightarrow 0$.*

Remark. *Assumption 1 is used to make sure the probability of accepting a worse case is low as the iteration increases (i.e., as the data gets closer to the truth). Additionally, the probability should be low if $\Delta^{(r)}$, the consequence of accepting a worse case is bad. The general idea of cov-Gen, as detailed in Subsection 2.3, is a modification of the simulated annealing algorithm. A reasonable choice of f that satisfies Assumption 1 is $f(\Delta, \gamma) = \exp(-\Delta/\gamma)$. Recommended default values for R, H, a, b is provided as $R \simeq 1E6 - 2.5E7, H \approx 1\%, a \geq 1, b \leq 20$. For each step, a random number of indices is swapped. If $b - a$ is large, then a large number of indices are changed each step, and the procedure stabilizes very slowly. A general recommendation is to adaptively reduce both a and b as the loss become smaller. The idea is simple but complicates the algorithm significantly, hence we omit the details for simplicity.*

The number of iterations R is not specified and can be arbitrarily large. In practice, the iterations needed to reach a relative loss $\mathcal{L}_m \leq 2\%$ while controlling $\mathcal{L}_{HR} \leq 1\%$ is usually around $1E6 - 1E7$ repetitions, but it highly depends on the quality of digitization. Instead of requiring the number of iterations R , the procedure can be carried out by specifying upper bounds on the RAEs, i.e., ‘stop if $\mathcal{L}_m \leq \tau_m\%$ (resp. $\mathcal{L}_m \leq \tau_{HR}\%$)’. Then, the algorithm has hyper-parameters $(\tau_m, \tau_{HR}, H, a, b)$. In general, \mathcal{L}_{HR} is easier to control than \mathcal{L}_m . Thus, we only require \mathcal{L}_{HR} to be upper bounded by some pre-specified threshold, say $H = 1\%$, and allow for small perturbations, while sequentially minimizing over \mathcal{L}_m .

2.3 Optimization, simulated annealing and interpretations

The simulated annealing (SA) is a probabilistic technique for approximating the global optimum of a given function, which is typically used for addressing complex global optimization problems whose objective function may be complex and can only be evaluated via some costly computer simulation [20, 4].

Let i be one possible state of the solution, let S_i be the neighborhood of i . Let r be the current iteration and $t^{(r)}$ be the value of the temperature parameter, where it gets the name from the algorithm's close relation to the physical annealing of materials [5, Section 2.3]. In brief, the SA algorithm starts with an initial state $i^{(0)}$, for the r th repetition, it generates $j^{(r)} \in S_{i^{(r)}}$, compares the value of the objective function h , and moves to state $j^{(r)}$ with probability

$$P(\text{accept } j^{(r)}) = \begin{cases} 1, & \text{if } h(j^{(r)}) < h(i^{(r)}), \\ \exp\left(\frac{h(i^{(r)}) - h(j^{(r)})}{t^{(r)}}\right), & \text{else,} \end{cases} \quad (3)$$

where $\lim_{r \rightarrow \infty} t^{(r)} = 0$. The decreasing sequence of $t^{(r)}$ is used to control the evolution of the system. For sufficiently small values of $t^{(r)}$, the system will then increasingly favor moves that go ‘downhill’ (i.e., achieves smaller loss), and avoid those that go ‘uphill’. With $t^{(r)} \equiv 0$ the procedure reduces to the greedy algorithm, which makes only the downhill transitions. Instead of using exponential decay in Equation (3), we generalize to function f under Assumption 1 in our method. For a more detailed description of the algorithm, see [5, 47] therein.

We now state the problem as a constrained optimization problem and relate Algorithm 2.2.2 to the SA algorithm. Given $\tilde{d}_n^{(-x)}, d_n$, the cov-Gen method is essentially solving for

the following complex constrained optimization problem:

$$\begin{aligned} \tilde{\mathbf{x}} = \operatorname{argmin}_{\mathbf{x} \in \{0, \dots, K\}^n} \mathcal{L}_m \left\{ (\tilde{d}_n^{(-x)}, \mathbf{x}) \mid d_n \right\}, \\ \text{subject to } \mathcal{L}_{\text{HR}} \left\{ (\tilde{d}_n^{(-x)}, \mathbf{x}) \mid d_n \right\} \leq H\%, \sum_{i=1}^n \mathbb{1}\{x_i = x, a_i = a\} = n_{x,a} \quad \forall x, a. \end{aligned} \quad (4)$$

Problem (4) is complex and to the best of our knowledge, may not admit a unique solution.

To apply the SA algorithm under our setup, the objective function is $\mathcal{L}_m \left\{ (\tilde{d}_n^{(-x)}, \mathbf{x}) \mid d_n \right\}$, the neighborhood of \mathbf{x} is defined as $\mathbf{x}' \in \{0, \dots, K\}$ such that at least $a\%$, at most $b\%$ of the coordinates within the same subgroup class are swapped. The coordinates are swapped with probability 1 if the median error enjoys a reduction, that is,

$$\mathcal{L}_m \left\{ (\tilde{d}_n^{(-x)}, \mathbf{x}) \mid d_n \right\} - \mathcal{L}_m \left\{ (\tilde{d}_n^{(-x)}, \mathbf{x}') \mid d_n \right\} > 0.$$

Moreover, if $f(\cdot, 0) \equiv 0$ in Algorithm 2.2.2 then, the cov-Gen reduces to a randomized local search [47, Algorithm 1]. We adopt the idea of traversing the solution plane by considering neighborhoods and accept worse case with low probability. One subtle difference, however, is that cov-Gen does not introduce the temperature parameter $t^{(r)}$. The cov-Gen method can be seen as a modified version of the SA algorithm with additional relaxations on the definition of neighbors, temperature and transition probability functions.

Problem (4) minimizes \mathcal{L}_m subject to a constraint over the magnitude of \mathcal{L}_{HR} and the number of subjects. In survival analysis, median survival typically controls the event/censoring behavior. The HR describes the difference between two survival curves (treatment vs control). Our motivation originates from the simultaneous control over the loss of median survival, HR, together with CI's. Such control guarantees the behavior of the two KM curves and the synthetic data to be similar to the original data.

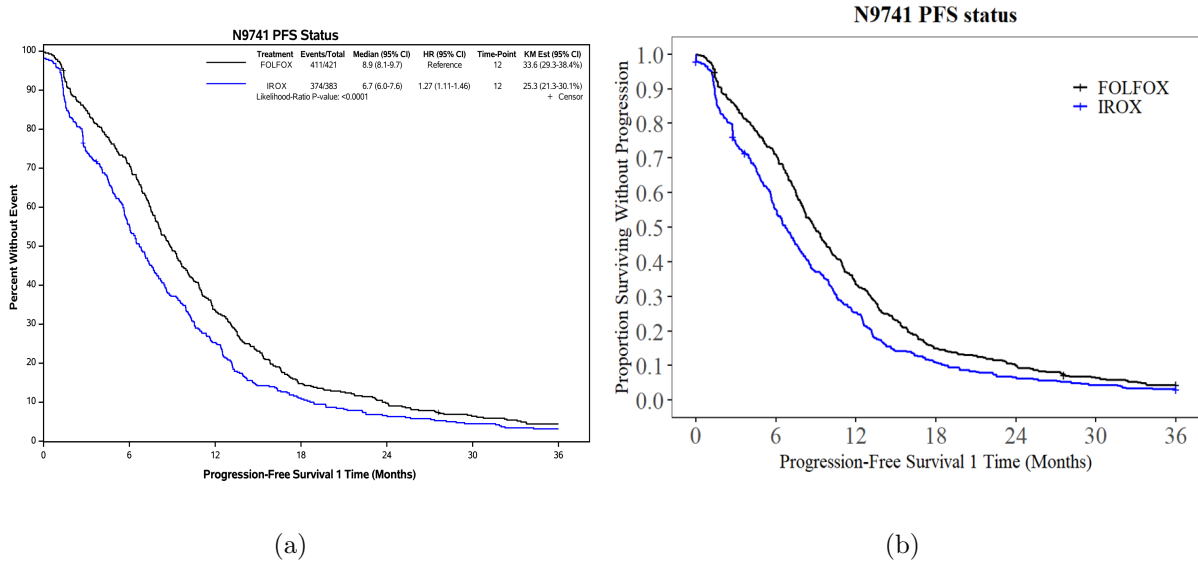


Figure 4: (a) True KM plots (all randomized patients) $\mathcal{G}_1, \mathcal{G}_0$ with $\mathcal{T} = \{0, 6, 12, \dots, 36\}, \mathcal{N}_1 = \{421, 298, \dots, 18\}, \mathcal{N}_0 = \{383, 210, \dots, 12\}$; (b) Synthetic KM plot (all randomized patients) for N9741 study.

3 Application and case studies

3.1 Application to statistical insight discovery

3.1.1 The N9741 data and methods

N9741 [12] is a clinical trial targeting patients with metastatic colorectal cancer. Among randomized patients, 421 were randomized to receive FOLFOX (oxaliplatin+fluorouracil+leucovorin) and 383 were randomized to receive IROX (irinotecan+oxaliplatin). The KM plots of all randomized patients are given in Figure 4 and the partial subgroup analysis table is provided in Table 2. These values are generated by d_n and no other information is given to us.

3.1.2 Results

Gaining statistical insights: The KM plot for all randomized patients (Figure 4) is first digitized using DIGITIZE($\mathcal{G}_a, \mathcal{N}_a, \mathcal{T} : a \in \{0, 1\}$) algorithm, then synthetic covariates are generated by cov-Gen($\tilde{d}_n^{(-x)}, \hat{\mathcal{J}}_{m_{x,a}}, \hat{\mathcal{J}}_{\widehat{\text{HR}}_x}, \hat{\mathcal{J}}_{\widehat{\text{sr}}_{x,a}}^{(12)}; 2.5E7, 2\%, 1, 20, f \equiv 0$), where $\text{sr}_{x,a}^{(12)}$ is the function calculating survival rates at month 12 for each subgroup. The data are then combined and the subgroup analysis table based on \tilde{d}_n is shown in Table 2. It is almost identical to Table 2 with slight underestimation of event numbers. This is mainly because the grids $\mathcal{N}_1, \mathcal{N}_0$ ends with a positive number of patients at risk (18 and 12, see Figure 4), the algorithm treats them automatically as censorings. Therefore, the median PFS and HR may be overestimated a little. Figure 5 reports the KM curves for each of the 4 subgroups considered. The KM lines of the synthetic IPD aligns closely with the truth. Additionally, the survival rates at 12 months for each subgroup using d_n and using \tilde{d}_n are calculated, the results show $\mathcal{L}_{\text{sr}^{(12)}}(\tilde{d}_n | d_n) \leq 0.5\%$.

3.2 Application to establishing benchmark survival and validating aggregated analysis

3.2.1 Data and methods

The proposed algorithm is used to validate a meta-analysis result on daratumumab for MM. In [11], the addition of Daratumumab to MM regimens is evaluated in high-risk cytogenetic patients to identify if such addition is associated with improved survival outcome. Six studies are identified to be eligible after screening. We retrieve the hazard ratios in high-risk cytogenetic subgroup reported for each study, see Table 3 and conduct a trial-level random effect meta-analysis to find the overall effect of Daratumumab in cytogenetic high-risk MM patients. Additionally, since the eligible studies all satisfy conditions for the

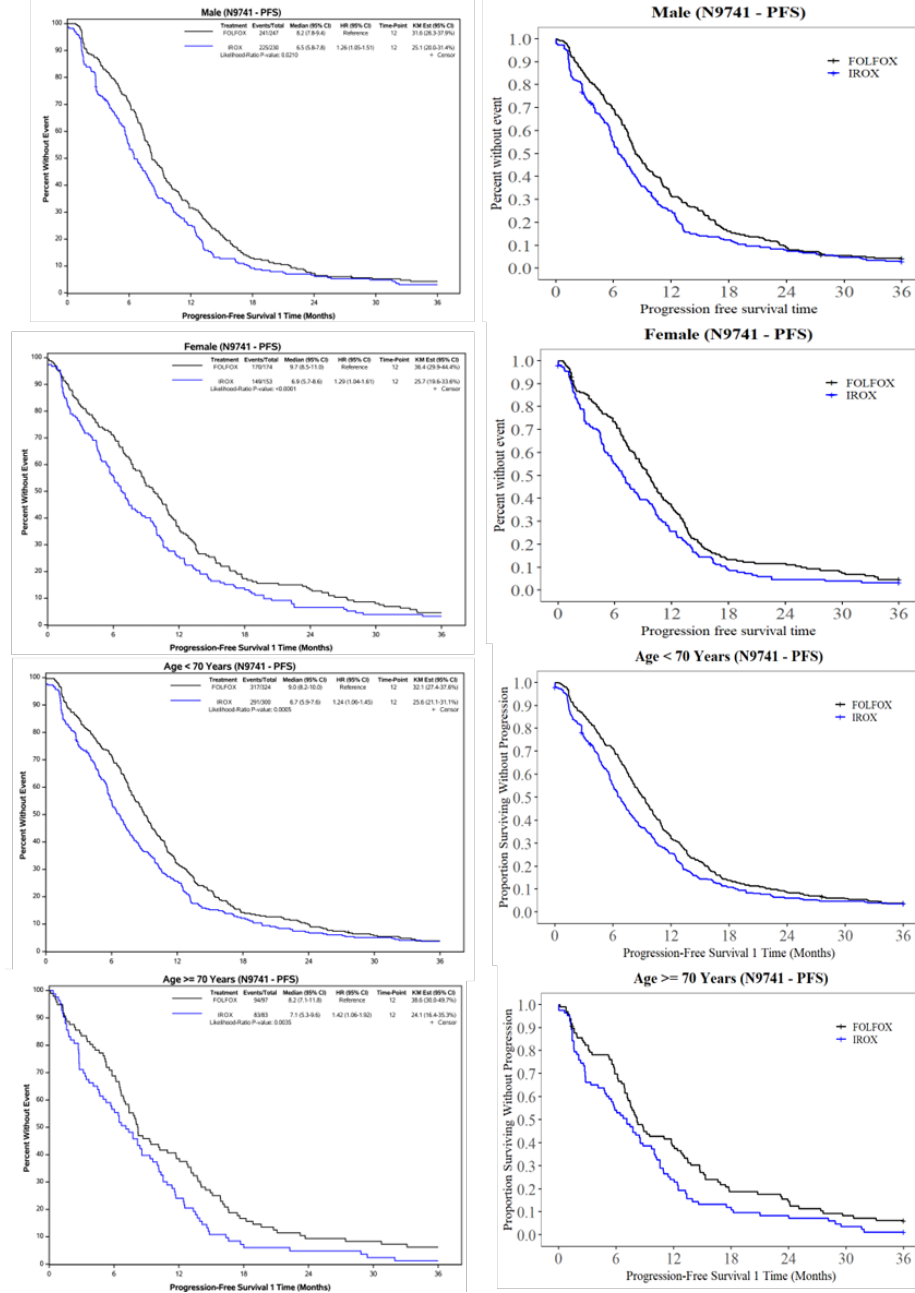


Figure 5: The subgroup KM plots for N9741 study. The left 4 plots are generated by d_n , the right 4 plots are generated by \tilde{d}_n . Two plots in the same row correspond to the same subgroup.

Table 2: Subgroup analysis table for N9741 study. *: reported by SynthIPD

| | FOLFOX ($n = 421$) | | IROX ($n = 383$) | | HR (95% CI) |
|----------------|----------------------|---------------------|--------------------|---------------------|------------------|
| | Events/Total | Median PFS (95% CI) | Events/Total | Median PFS (95% CI) | IROX vs FOLFOX |
| Gender | | | | | |
| Male | 241/247 | 8.2 (7.8-9.4) | 225/230 | 6.5(5.8-7.8) | 1.26(1.05-1.51) |
| Female | 170/174 | 9.7 (8.5-11.0) | 149/153 | 6.9(5.7-8.6) | 1.29(1.04-1.61) |
| Age | | | | | |
| Age < 70 | 317/324 | 9.0 (8.2-10.0) | 291/300 | 6.7 (5.9-7.6) | 1.24 (1.06-1.45) |
| Age \geq 70 | 94/97 | 8.2 (7.1-11.8) | 83/83 | 7.1 (5.3-9.6) | 1.42 (1.06-1.92) |
| Gender* | | | | | |
| Male | 241/247 | 8.2 (7.8-9.4) | 225/230 | 6.5(5.8-7.8) | 1.26(1.05-1.51) |
| Female | 170/174 | 9.7 (8.5-11.0) | 149/153 | 6.9(5.7-8.6) | 1.29(1.04-1.61) |
| Age* | | | | | |
| Age < 70 | 311/324 | 9.1 (8.2-10.1) | 286/300 | 6.7 (6.0-7.6) | 1.26 (1.07-1.47) |
| Age \geq 70 | 90/97 | 8.2 (7.2-12.1) | 82/83 | 7.1 (5.3-9.7) | 1.44 (1.06-1.94) |

implementation of our algorithm (see Figure 6), therefore, we reconstruct synthetic IPD for all 6 studies and then use cox models (stratified by study names) to calculate the overall hazard ratio, i.e., a meta analysis with IPD.

3.2.2 Results

Validating meta-analysis: SynthIPD for cytogenetic high-risk patients were generated for three studies for NDMM: ALCYONE [27], CASSIOPEIA [28], MAIA [9] (total sample size 2528); and three studies for RRMM: CANDOR [6], CASTOR [30], POLLUX [8] (total sample size 1533). The generated HRs for each study closely aligned with reported HRs for high-risk patients, with $\mathcal{L}_{\text{HR}} \leq 2\%$. By pooling these datasets, we obtained SynthIPD datasets for NDMM and RRMM patients. Stratified Cox regression analy-

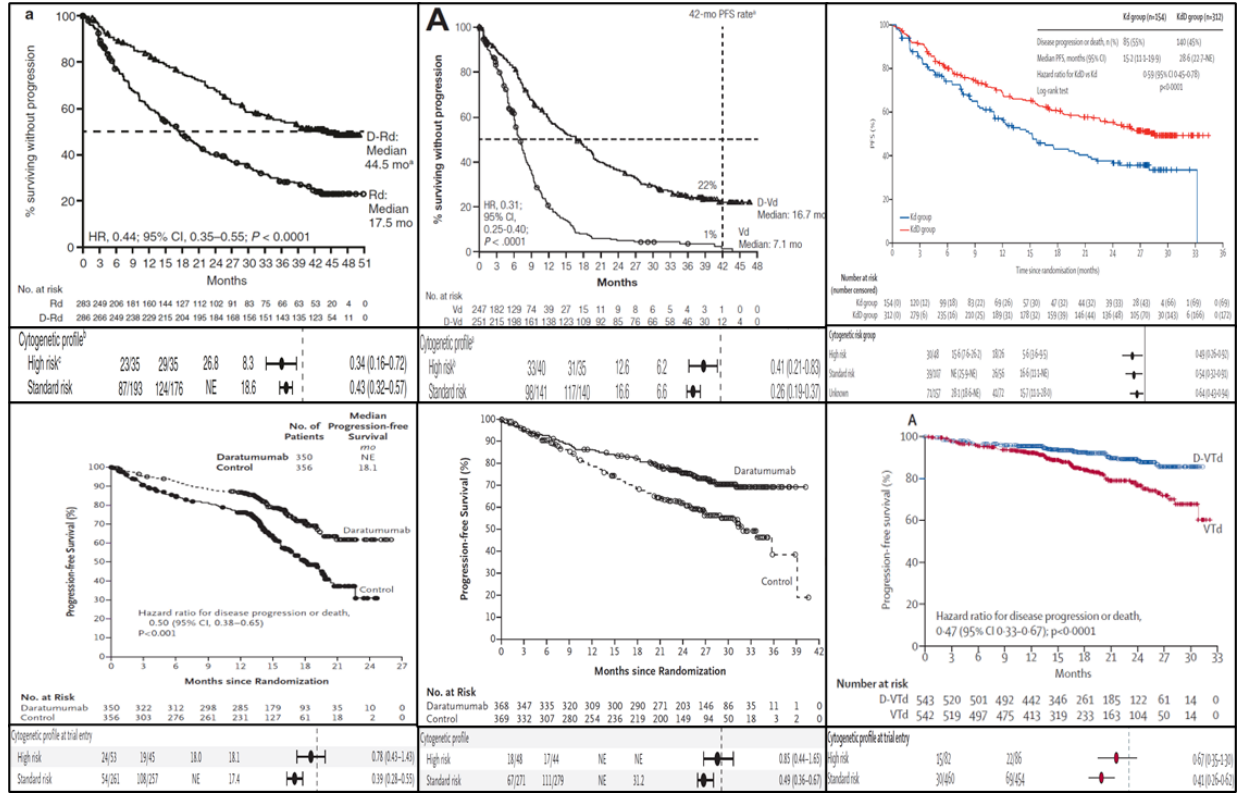


Figure 6: The information used to generate synthetic IPD. Top left: POLLUX ($n = 286$ vs 283), top middle: CASTOR ($n = 251$ vs 247), top right: Candor ($n = 312$ vs 154); bottom left: ALYCONe ($n = 356$ vs 350), bottom middle: MAIA ($n = 369$ vs 368), bottom right: CASSIOPEIA ($n = 543$ vs 542). The median survival and HR stratified by cytogenetic risk are attached below the KM plots $\mathcal{G}_1, \mathcal{G}_2$ for all cases.

Table 3: Reported event numbers and hazard ratios (Dara versus no Dara) in high-risk cytogenetic subgroup. NDMM: newly diagnosed MM, RRMM: relapsed or refractory MM.

| Disease population | Study popular name | n (Dara vs no Dara) | HR(95% CI) |
|--------------------|--------------------|-----------------------|------------------|
| NDMM | CASSIOPEIA [28] | 82 vs 86 | 0.67 (0.35-1.30) |
| | MAIA[9] | 48 vs 44 | 0.85 (0.44-1.65) |
| | ALYCONe [27] | 53 vs 45 | 0.78 (0.43-1.43) |
| RRMM | CANDOR [6] | 48 vs 26 | 0.49 (0.26-0.92) |
| | CASTOR [30] | 40 vs 35 | 0.41 (0.21-0.83) |
| | POLLUX [8] | 35 vs 35 | 0.34 (0.16-0.72) |

ses yield HRs of 0.76(95%CI 0.53 – 1.10) for NDMM and 0.43(95%CI 0.29 – 0.61) for RRMM. Random-effects meta-analyses show HRs of 0.76(95%CI 0.53 – 1.10) for NDMM and 0.43(95%CI 0.29 – 0.62) for RRMM. Compare with traditional meta-analysis techniques, the synthetic data approach provides additional clinical insights that were not available in the original publications. For instance, the clinical results for the six studies within high-risk group (e.g., KM curves in high-risk subgroup) can be reproduced, which are not reported in the original studies.

Establishing benchmark: Additionally, the data set ($n = 4061$) is pooled together and the benchmark median PFS for Daratumumab treated patients are established in Table 4. The median PFS in NDMM population are not estimable for most cases, indicating the necessity for a more sensitive surrogate endpoint when treated by Daratumumab. These benchmark results can be further used to guide the estimation of the sample size needed for a new Phase III clinical trial involving Daratumumab as placebo.

Table 4: The benchmark median PFS for patients treated by Daratumumab. §: The treatment for NDMM includes Dara-VTd, Dara-VMP, and Dara-Rd. †: The treatment for RRMM includes Dara-Vd, kdD, and Dara-Rd. NE: not estimable because the median PFS is not reached due to short follow-up.

| Cytogenetic risk | Disease population | Analyzed sample size | median PFS (95% CI) |
|------------------|--------------------|----------------------|---------------------|
| High | NDMM § | 183 | NE (24.2, NE) |
| | RRMM † | 123 | 16.9 (10.2, 23.7) |
| Standard | NDMM | 992 | NE (NE, NE) |
| | RRMM | 441 | 30.3 (26.5, 36.6) |
| Unknown | NDMM | 86 | NE (NE, NE) |
| | RRMM | 285 | 26.1 (23.1, 38.2) |

4 Simulation studies and evaluation

Some metrics are proposed to evaluate the DIGITIZE and cov-Gen methods, followed by simulation verifications. Suppose both d_n and \tilde{d}_n are available at hand, the following two metrics are useful.

Definition 1 (NAUC). *The NAUC in subgroup $X = x, A = a$ given d_n is defined as*

$$NAUC_{x,a}(\tilde{d}_n \mid d_n) := \frac{1}{\tau} \int_0^\tau |\hat{S}_{x,a}(t) - \tilde{S}_{x,a}(t)| dt \in [0, 1],$$

where $\tau > 0$ is a fixed time point, usually taken to be the largest event/censoring time.

Definition 2 (Kolmogorov-Smirnov distance). *The Kolmogorov-Smirnov distance in subgroup $X = x, A = a$ given d_n is defined as*

$$KS_{x,a}(\tilde{d}_n \mid d_n) := \sup_{0 \leq t \leq \tau} \left| \hat{S}_{x,a}(t) - \tilde{S}_{x,a}(t) \right| \in [0, \infty),$$

where $\tau > 0$ is a fixed time point, usually taken to be the largest event/censoring time.

NAUC measures the averaged discrepancy between survival distributions while K-S distance measures the single largest vertical gap between the survival curves introduced by true versus synthetic IPD. For fixed d_n, \tilde{d}_n , a smaller NAUC and/or K-S distance indicates a better synthetic copy.

Practically, both metric can be estimated using a discrete estimator. Suppose the distinct, ordered events up to time τ are $0 = t_{(0)} \leq \dots \leq t_{(q)} \leq \tau$ with $\delta_j = t_{(j)} - t_{(j-1)}, j \in [q]$, then

$$\widehat{\text{NAUC}}_{x,a}(\tilde{d}_n \mid d_n) := \frac{1}{\tau} \sum_{j=1}^q \delta_j \left| \hat{S}_{x,a}(t_{(j)}) - \tilde{S}_{x,a}(t_{(j)}) \right|, \quad \widehat{\text{KS}}_{x,a}(\tilde{d}_n \mid d_n) := \max_{1 \leq j \leq q} \left| \hat{S}_{x,a}(t_{(j)}) - \tilde{S}_{x,a}(t_{(j)}) \right|.$$

Finally, since there are K categories and 2 arms, $2K$ estimates will be produced for each metric for each synthetic data set. To see the integrated performance of \tilde{d}_n , it is reasonable to calculate the (weighted) average across different subgroups:

$$\widehat{\text{NAUC}}(\tilde{d}_n \mid d_n) := \sum_{x \in [K]} \sum_{a \in \{0,1\}} \frac{n_{x,a}}{n} \widehat{\text{NAUC}}_{x,a}(\tilde{d}_n \mid d_n), \quad \widehat{\text{KS}}(\tilde{d}_n \mid d_n) := \frac{1}{2K} \sum_{x \in [K]} \sum_{a \in \{0,1\}} \widehat{\text{KS}}_{x,a}(\tilde{d}_n \mid d_n).$$

The NAUC metric is weighted by the sample size because a larger number of observations may introduce larger NAUC value. Conversely, K-S distance is weighted equally because it measures the worst case scenario and each case is equally important.

In practice, d_n is usually not available. Thus, the evaluation through NAUC or K-S distance is not appropriate. One other to evaluate the proposed method is to directly compare the summary statistics (e.g., median survivals, hazard ratios, survival rates, and their confidence intervals, etc.) generated by \tilde{d}_n with that generated by d_n . For any summary statistics g , depending on its definition, the following maximum RAEs may be convenient for this purpose

$$\mathcal{L}_g(\tilde{d}_n \mid d_n) = \max_{x,a} \left| \frac{\hat{g}_{x,a}(d_{n,x,a}) - \hat{g}_{x,a}(\tilde{d}_{n,x,a})}{\hat{g}_{x,a}(d_{n,x,a})} \right|,$$

$$\mathcal{L}_g(\tilde{d}_n \mid d_n) = \max_x \left| \frac{\hat{g}_x(d_{n,x}) - \hat{g}_x(\tilde{d}_{n,x})}{\hat{g}_x(d_{n,x})} \right|.$$

The two losses are essentially equivalent to Equations (1),(2) if $g = m$ or $g = \text{HR}$, and can be applied other statistics as well. Note that the calculation of \mathcal{L}_g requires the summary statistics $\hat{g}_{x,a}(d_{n,x,a})$ or $\hat{g}_x(d_{n,x})$, to be reported in the original publication. From our experience, the survival rates $g = \text{sr}$ may be available from time to time. In the most limited case, $\mathcal{L}_m, \mathcal{L}_{\text{HR}}$ would be available due to our requirements in Section 2.

4.1 Evaluation of DIGITIZE

In this section, we compare $\text{DIGITIZE}(\mathcal{G}_a, \mathcal{N}_a, \mathcal{T} : a \in \{0, 1\})$ with the existing digitization method, IPDfromKM [23]. The data of size $n = 500$ is generated using CASE 1 in Subsection 4.1.

Table 5 shows the summary statistics generated by the true data generating mechanism, the SynthIPD (DIGITIZE) method and the IPDfromKM method respectively. Figure 7 (in Appendix A) presents the KM plots drawn by these three data sets independently. From both Table and Figure, we see that DIGITIZE method produces synthetic data with higher precision, in terms of capturing the position of censoring in KM plot and retrieving the statistic values. This is expected since we can extract exact coordinates from the SVG plots, while IPDfromKM suffers from manual digitization error.

4.2 Evaluation of cov-Gen

To evaluate the performance of cov-Gen, we simulate IPD from different data generating mechanisms and assume the digitization is done without error, that is, $\tilde{u}_i = u_i, \tilde{\delta}_i = \delta_i, \tilde{a}_i = a_i$ for every $i \in [n]$, and we generate \tilde{x}_i only so that $\tilde{d}_n = \{u_i, \delta_i, a_i, \tilde{x}_i\}_{i=1}^n$. Since the original IPD d_n is known from simulation, the performance can be evaluated via all evaluation methods proposed. For each of the 100 repetitions considered, the number

Table 5: The comparison of summary statistics with different methods for generating ITT data.

| Method | Treatment | n/events | median PFS (95% CI) | HR(95% CI) |
|-----------|-----------|----------|---------------------|------------------|
| Truth | Treatment | 227/121 | 22.55(16.37-26.93) | 0.21 (0.16-0.26) |
| | Control | 273/224 | 3.55(3.08-4.34) | Reference level |
| IPDfromKM | Treatment | 227/119 | 22.83(16.52-27.02) | 0.21(0.16-0.27) |
| | Control | 273/220 | 3.95(3.09-4.43) | Reference level |
| SynthIPD | Treatment | 227/121 | 22.55(16.37-26.93) | 0.21 (0.16-0.27) |
| | Control | 273/224 | 3.55(3.08-4.34) | Reference level |

of patients are set to $n = 500$, and are randomly assigned to active treatment or control group with equal probability. The following three data generating mechanisms are considered and $\text{cov-Gen}(\tilde{d}_{500}^{(-x)}, \hat{\mathcal{J}}_{\hat{m}_{x,a}}, \hat{\mathcal{J}}_{\widehat{\text{HR}}_x}; 2.5E6, 1\%, 5, 20, f)$ is used for each case, where $f(\Delta, \gamma) = \exp(-\Delta/\gamma)$.

CASE 1. (Proportional hazard model) Consider two covariates $X_{i,1}, X_{i,2}$ both simulated independently and identically from Bernoulli(0.3) distributions. The responses are generated from a cox proportional hazard model

$$\lambda(t \mid A_i, \mathbf{X}_i) = \frac{\log(2)}{10} \exp(\log(0.7)A_i + \log(0.5)X_{i,1} + \log(0.75)X_{i,2}).$$

CASE 2. (AFT model) Let the two covariates $X_{i,1}, X_{i,2}$ be independent random variables from Bernoulli(0.3), Bernoulli(0.4) respectively. The event time follows an accelerated event time model $\log(T_i) = 0.8A_i - 0.7X_{i,1} + 0.5X_{i,2} + \varepsilon_i$ where $\varepsilon_i \sim \mathcal{N}(0, 0.3^2)$.

CASE 3. (Cross-over) Consider two covariates $X_{i,1}, X_{i,2}$ both simulated independently and identically from Bernoulli(0.3) distributions. Consider a case under which the baseline hazards vary by time. Specifically, set $t_0 = 5$, the baseline hazard for group a is defined as

$$\lambda_a(t) = 0.1\mathbb{1}\{a = 0, t < t_0\} + 0.2\mathbb{1}\{a = 1, t < t_0\} + 0.3\mathbb{1}\{a = 0, t \geq t_0\} + 0.1\mathbb{1}\{a = 1, t \geq t_0\}$$

where $\mathbb{1}(\cdot)$ is the indicator function. The individual hazard function is then defined as $\lambda(t \mid A_i = a, \mathbf{X}_i) = \lambda_a(t) \exp(\log(1.8)X_{i,1} + \log(0.5)X_{i,2})$.

CASE 1 examines the popular cox model, CASE 2 studies the acceleration failure time model, under which the cox assumption is violated. CASE 3 investigates a complex scenario where there is a cross-over in survival time, i.e., the KM plots for the two treatment groups intersect at one or more time points. For each case, the censoring times will be generated by an exponential distribution such that the censoring rate is between 30% – 50%.

Table 6 reports the mean of the evaluation metrics $\widehat{\text{NAUC}}$, $\widehat{\text{KS}}$, \mathcal{L}_m and \mathcal{L}_{HR} discussed over 100 repetitions across both margins $X_{i,1}$, $X_{i,2}$ and strata $(X_{i,1}, X_{i,2})$. The small magnitude of NAUC (resp. K-S distance) indicates the KM curves for true IPD and synthIPD are close on average (resp. on average in the worst case scenario). For each case, the $\mathcal{L}_m, \mathcal{L}_{\text{HR}}$ are also low on average, which implies SynthIPD generates data with similar properties as the true IPD. Additionally, A KM graphic comparison for CASE 2 is presented in Appendix A.

Table 6: For each case, the mean of $\widehat{\text{NAUC}}$, $\widehat{\text{KS}}$, $\mathcal{L}_m(\tilde{d}_n)$, and $\mathcal{L}_{\text{HR}}(\tilde{d}_n)$ are reported.

| Case | Subgroup | $\widehat{\text{NAUC}}$ | $\widehat{\text{KS}}$ | $\bar{\mathcal{L}}_m(\tilde{d}_n)$ | $\bar{\mathcal{L}}_{\text{HR}}(\tilde{d}_n)$ |
|--------|----------------------|-------------------------|-----------------------|------------------------------------|--|
| CASE 1 | $X_{i,1}$ | 2.0E-2 | 6.9E-2 | 3.0E-2 | 1.5E-1 |
| | $X_{i,2}$ | 2.3E-2 | 7.4E-2 | 1.0E-2 | 6.0E-3 |
| | $(X_{i,1}, X_{i,2})$ | 1.8E-2 | 7.0E-2 | 2.0E-2 | 1.0E-1 |
| CASE 2 | $X_{i,1}$ | 8.7E-3 | 2.7E-2 | 2.0E-3 | 4.0E-3 |
| | $X_{i,2}$ | 8.7E-2 | 2.9E-2 | 4.0E-2 | 3.8E-3 |
| | $(X_{i,1}, X_{i,2})$ | 7.5E-3 | 2.5E-2 | 4.3E-2 | 3.5E-3 |
| CASE 3 | $X_{i,1}$ | 1.8E-2 | 6.4E-2 | 4.0E-2 | 4.0E-3 |
| | $X_{i,2}$ | 2.1E-2 | 4.3E-2 | 5.2E-2 | 2.6E-2 |
| | $(X_{i,1}, X_{i,2})$ | 2.2E-2 | 5.3E-2 | 4.1E-2 | 3.0E-3 |

4.3 SynthIPD as pseudo IPD

To demonstrate the effectiveness of SynthIPD versus existing approaches and its potential to serve as pseudo-training sets for other generative models, we conduct comparisons on both real and simulated data, using survivalGAN (Python package `synthcity`) [29] and decision tree methods (R package `synthpop`) [2].

Comparison with other methods: The Rotterdam tumor bank dataset [10] containing records for $n = 1546$ patients with node-positive breast cancer, combined with data from the German Breast Cancer Study Group [37] containing $n = 686$ patients is used. The combined survival data set, denoted d_{2232} , is described in [19, Section 4.5.2]. SurvivalGAN and Conditional decision trees are trained based on 7 covariates containing both categorical and continuous covariates, producing $\tilde{d}_{2232}^{\text{GAN}}, \tilde{d}_{2232}^{\text{tree}}$. In parallel, since SynthIPD handles categorical univariate covariate, it is applied to generate synthetic data sets for the three levels of the first covariate, producing $\tilde{d}_{2232,0}^{\text{SynthIPD}}, \dots, \tilde{d}_{2232,2}^{\text{SynthIPD}}$ (the subscript $0, \dots, 2$ denotes which margin of the covariate is used).

The real data results, summarized in Table 7, demonstrate that SynthIPD consistently outperforms survivalGAN across all evaluation metrics stratified by univariate covariate. Notably, SynthIPD achieves approximately $\approx 90\%$ (resp. $\approx 50\%$) relative improvement in NAUC and $\approx 80\%$ (resp. $\approx 50\%$) relative improvement in KS compared to survivalGAN (resp. conditional tree). SynthIPD also produces median survival summary statistics that is closer to the truth. Graphical illustration for the comparison of the three method will be provided in Appendix A.

Serving as pseudo training set: For the simulation based study, CASE 1 in Subsection 4.2 is used to generate the true IPD, then SynthIPD is used to generate survival time $\tilde{u}_i, \tilde{\delta}_i$ treatments \tilde{a}_i and covariates $\tilde{x}_{i,1}, \tilde{x}_{i,2}, i \in [500]$. SurvivalGAN and conditional tree models

Table 7: The metrics evaluated for $\tilde{d}_{2232}^{\text{GAN}}$, $\tilde{d}_{2232}^{\text{Tree}}$ and $\tilde{d}_{2232,0}^{\text{SynthIPD}}$, $\tilde{d}_{2232,1}^{\text{SynthIPD}}$, $\tilde{d}_{2232,2}^{\text{SynthIPD}}$ compared with truth d_{2232} .[†]: The error \mathcal{L}_m can be made arbitrarily small in principle at the expense of computation efficiency, i.e., letting $R \rightarrow \infty$.

| Method | Subgroup | $\widehat{\text{NAUC}}$ | $\widehat{\text{KS}}$ | $\mathcal{L}_m(\tilde{d}_{2232} \mid d_{2232})$ |
|------------------|----------|-------------------------|-----------------------|---|
| SurvivalGAN | $X = 0$ | 4.3E-2 | 8.1E-2 | 2.2E-1 |
| | $X = 1$ | 4.9E-2 | 9.6E-2 | 2.6E-1 |
| | $X = 2$ | 6.2E-2 | 1.1E-1 | 9.6E-2 |
| Conditional Tree | $X = 0$ | 8.6E-3 | 2.2E-2 | 1.5E-4 |
| | $X = 1$ | 7.0E-3 | 2.5E-2 | 2.6E-1 |
| | $X = 2$ | 1.9E-2 | 1.6E-1 | 9.6E-2 |
| SynthIPD | $X = 0$ | 4.5E-3 | 2.0E-2 | 1.0E-2 [†] |
| | $X = 1$ | 2.7E-3 | 1.0E-2 | 9.5E-3 |
| | $X = 2$ | 5.8E-3 | 2.3E-2 | 4.8E-3 |

are trained by

$$(u_i, \delta_i) \sim a_i + x_{i,1} + x_{i,2}, \quad (5)$$

$$(\tilde{u}_i, \tilde{\delta}_i) \sim \tilde{a}_i + \tilde{x}_{i,1} + \tilde{x}_{i,2}. \quad (6)$$

Then, the synthetic data generated by models (5) and (6) are compared with true IPD respectively. Notably, the relative difference in errors between models are less than 1%, i.e., if we observe under model (5), $\mathcal{L}_m(\tilde{d}_n^{\text{Model (5)}} \mid d_n) \approx 0.1$, then under model (6), $\mathcal{L}_m(\tilde{d}_n^{\text{Model (6)}} \mid d_n) \in (0.09, 0.11)$. This indicates the generative models with SynthIPD as training sets achieves the same performance as generative models with true IPD as training sets. Such observation unlocks the strong potential of using generative methods even without the access to true IPD.

Aside from any comparisons made, we stress that our method utilized only KM curves and summary statistics from published articles, while the other methods require true IPD to

train. In summary, this comparison indicates that our assumption-lean approach provides superior fidelity to the original data distribution.

5 Discussion

This work introduces a three-step algorithm that reconstructs synthetic IPD only based on published KM plots and subgroup summary statistics, bridging the gap between IPD and the privacy constraints that often preclude data sharing. If the practical requirements are met, the procedure reproduces each arm’s survival curve and covariates that match subgroup median survival and HRs within prespecified tolerances. The simulation experiments and real-world case studies demonstrate that these features translate into negligible error and effect estimates nearly identical from analyses based on the original data.

The proposed method shows promise in practice. The algorithm, as we see in simulation, can potentially be generalized to handle multivariate categorical covariates (stratum) as long as the related summary statistics are reported in the main article. Several directions for future work remain open. First, developing some theoretical results on convergence [16] and time complexity [36] of the annealing procedure would greatly improve the method’s reliability. Additionally, incorporating observational data through machine learning methods could extend the approach to handle covariates of higher dimensions instead of restricting to publications. Lastly, many parts of our algorithm currently require manual data extraction, especially the DIGITIZE step. Automating this process would significantly enhance its practical usefulness. These areas are left for future research.

A Additional simulation figures

Figure 7 compares the DIGITIZE method and the IPDfromKM [23] method graphically. Using our method, the KM curves are indistinguishable with the true curve. IPDfromKM produces similar trends but is not pointwisely accurate.

In Figures 8 (CASE 2) and Figure 9 (CASE 3), the IPD and synthetic IPD for the 100 repetitions are pooled together, resulting in $5E4$ observations in total. The KM curves are plotted side-by-side and there is no distinction except for a slight difference in the tail censoring behaviors.

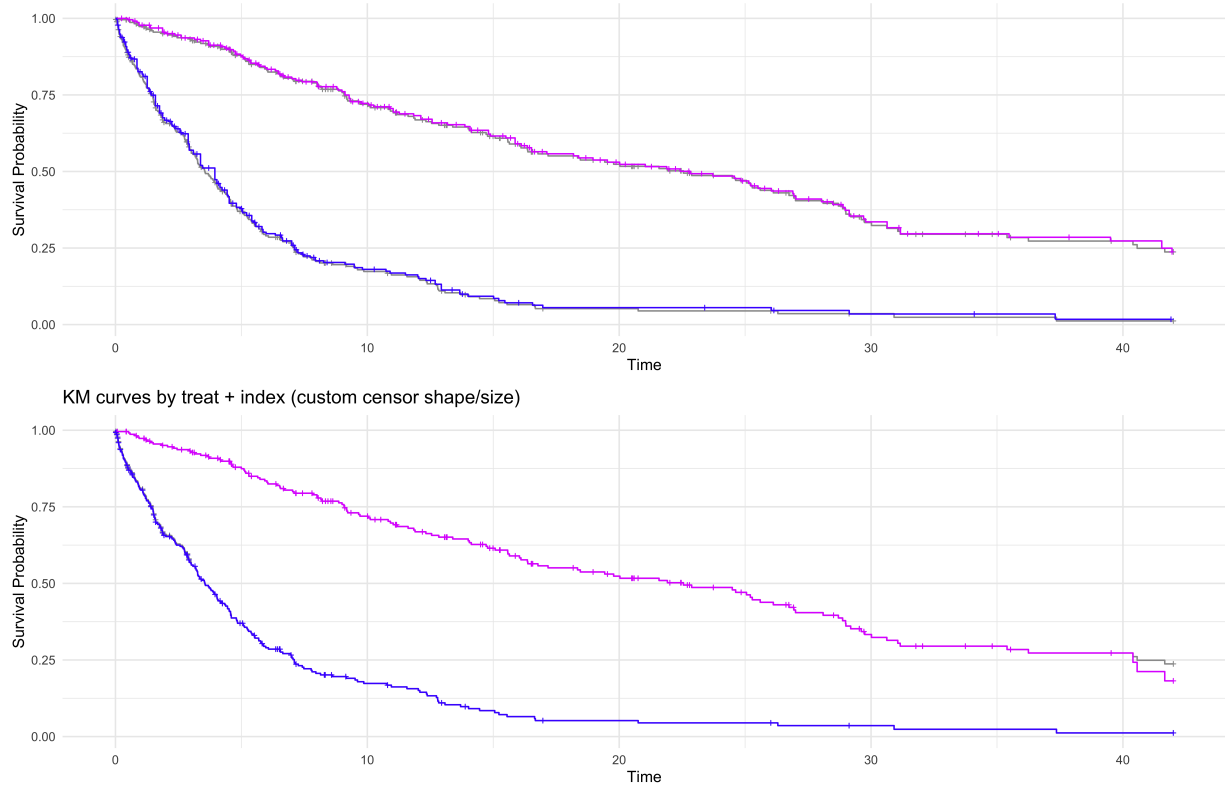


Figure 7: Comparison of DIGITIZE by SynthIPD and IPDfromKM method. The top plot is generated by IPDfromKM. The bottom plot is the result of DIGITIZE, the first step of SynthIPD. For each plot, the gray lines are the true KM curves.

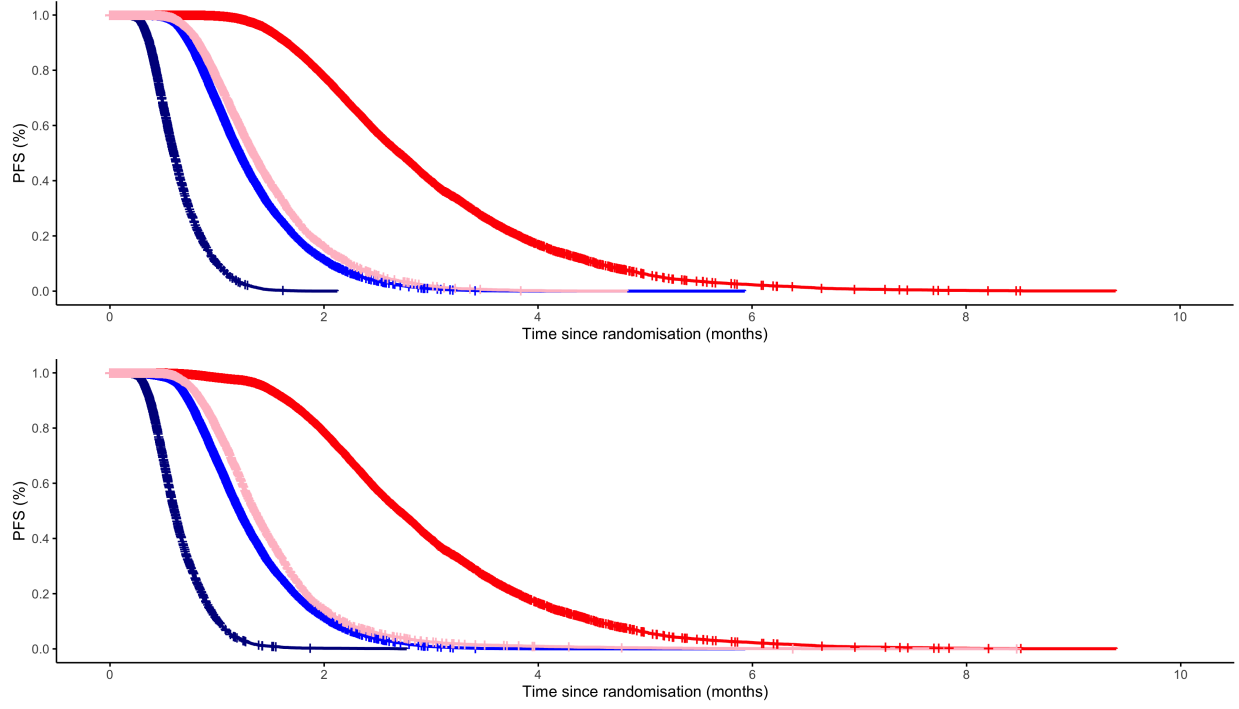


Figure 8: The IPD and synthetic IPD from 100 repetitions are pooled together and we report the KM PFS plot of pooled IPD (top figure) and pooled synthetic IPD (bottom figure) for CASE 2 stratified by treatment and covariate $X_{i,1}$. The red line represents $a = 1, x = 0$; the pink line represents $a = 1, x = 1$; the light blue line represents $a = 0, x = 0$; the dark blue line represents $a = 0, x = 1$.

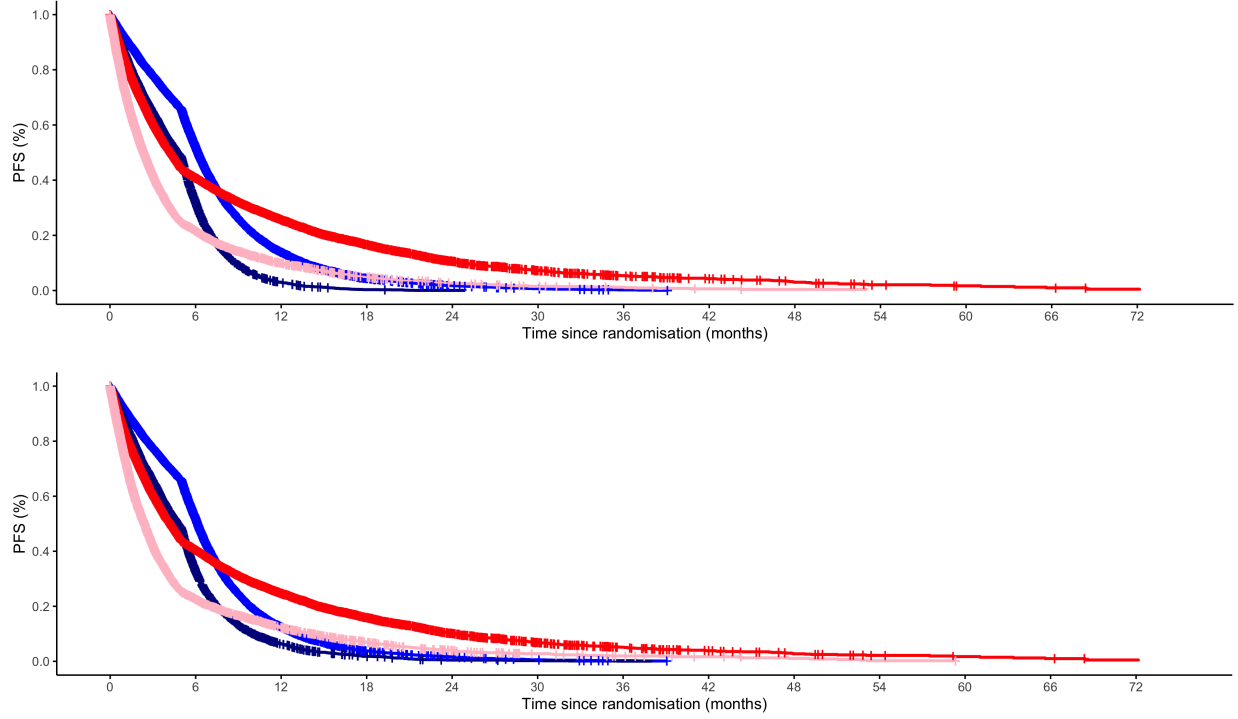


Figure 9: The IPD and synthetic IPD from 100 repetitions are pooled together and we report the KM PFS plot of pooled IPD (top figure) and pooled synthetic IPD (bottom figure) for CASE 3 stratified by treatment and covariate $X_{i,1}$. The red line represents $a = 1, x = 0$; the pink line represents $a = 1, x = 1$; the light blue line represents $a = 0, x = 0$; the dark blue line represents $a = 0, x = 1$.

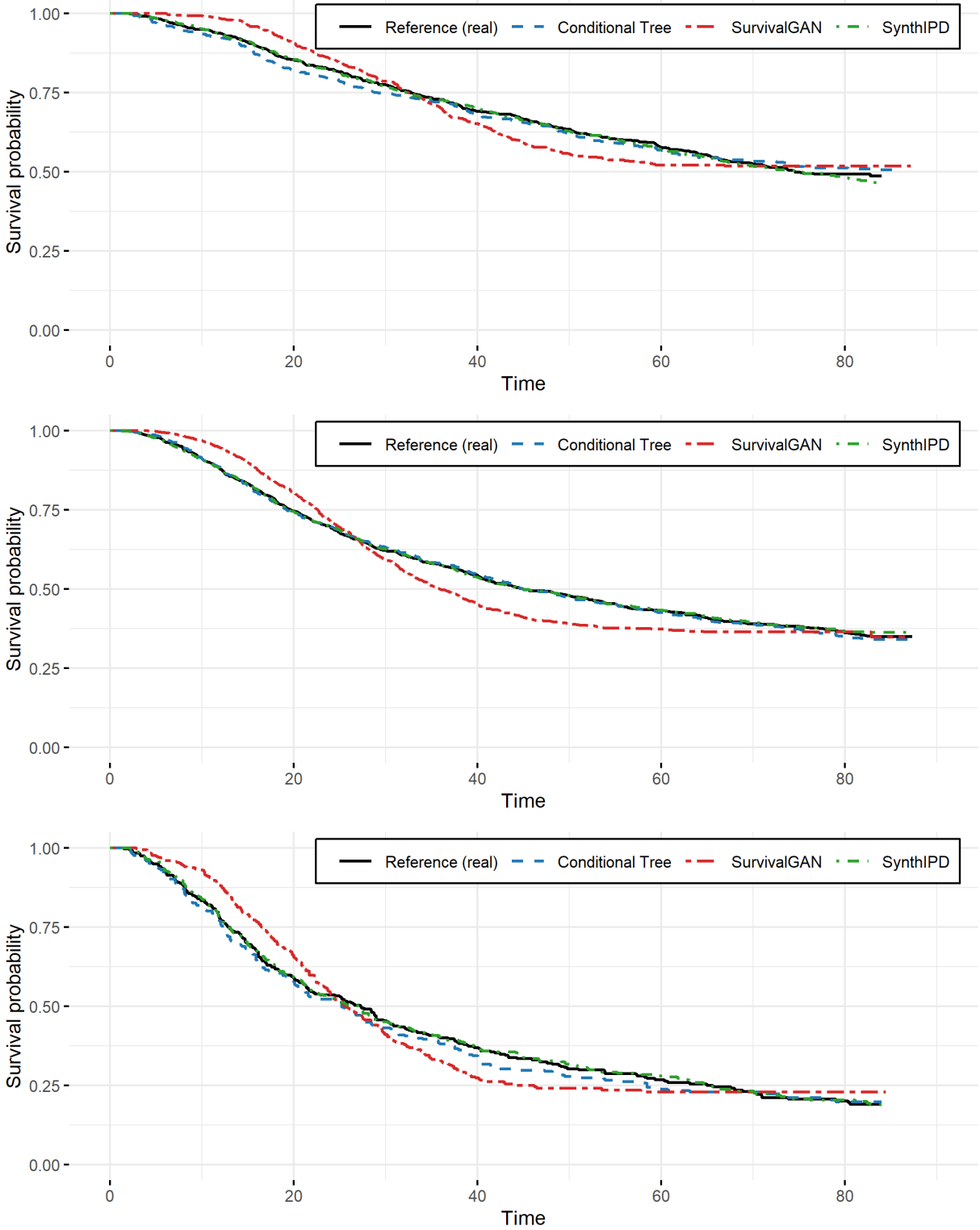


Figure 10: The comparison of KM curves for three synthetic data generating methods in Subsection 4.2. The three graphs correspond to subgroups $X = 0, 1, 2$ respectively from top to bottom.

References

- [1] Synthetic data generation methods in healthcare: A review on open-source tools and methods. Computational and Structural Biotechnology Journal, 23:2892–2910, 2024.
- [2] Zahra Azizi, Chaoyi Zheng, Lucy Mosquera, Louise Pilote, and Khaled El Emam. Can synthetic data be a proxy for real clinical trial data? a validation study. BMJ open, 11(4):e043497, 2021.
- [3] Scott M Berry, Bradley P Carlin, J Jack Lee, and Peter Muller. Bayesian adaptive methods for clinical trials. CRC press, 2010.
- [4] Dimitris Bertsimas and John Tsitsiklis. Simulated annealing. Statistical science, 8(1):10–15, 1993.
- [5] Daniel Delahaye, Supatcha Chaimatanan, and Marcel Mongeau. Simulated annealing: From basics to applications. In Handbook of metaheuristics, pages 1–35. Springer, 2018.
- [6] Meletios Dimopoulos, Hang Quach, Maria-Victoria Mateos, Ola Landgren, Xavier Leleu, David Siegel, Katja Weisel, Hui Yang, Zandra Klippel, Anita Zahlten-Kumeli, et al. Carfilzomib, dexamethasone, and daratumumab versus carfilzomib and dexamethasone for patients with relapsed or refractory multiple myeloma (candor): results from a randomised, multicentre, open-label, phase 3 study. The Lancet, 396(10245):186–197, 2020.
- [7] Meletios A Dimopoulos, Ruben Niesvizky, Katja Weisel, David S Siegel, Roman Hajek, María-Victoria Mateos, Michele Cavo, Mei Huang, Anita Zahlten-Kumeli, and Philippe Moreau. Once-versus twice-weekly carfilzomib in relapsed and refractory

- multiple myeloma by select patient characteristics: phase 3 arrow study subgroup analysis. Blood cancer journal, 10(3):35, 2020.
- [8] Meletios A Dimopoulos, Albert Oriol, Hareth Nahi, Jesus San-Miguel, Nizar J Bahlis, Saad Z Usmani, Neil Rabin, Robert Z Orlowski, Mieczyslaw Komarnicki, Kenshi Suzuki, et al. Daratumumab, lenalidomide, and dexamethasone for multiple myeloma. New England Journal of Medicine, 375(14):1319–1331, 2016.
- [9] Thierry Facon, Shaji Kumar, Torben Plesner, Robert Z Orlowski, Philippe Moreau, Nizar Bahlis, Supratik Basu, Hareth Nahi, Cyrille Hulin, Hang Quach, et al. Daratumumab plus lenalidomide and dexamethasone for untreated myeloma. New England Journal of Medicine, 380(22):2104–2115, 2019.
- [10] John A Foekens, Harry A Peters, Maxime P Look, Henk Portengen, Manfred Schmitt, Michael D Kramer, Nils Brunner, Fritz Janicke, Marion E Meijer-van Gelder, Sonja C Henzen-Logmans, et al. The urokinase system of plasminogen activation and prognosis in 2780 breast cancer patients. Cancer research, 60(3):636–643, 2000.
- [11] Smith Giri, Alyssa Grimshaw, Susan Bal, Kelly Godby, Prakash Kharel, Benjamin Djulbegovic, Meletios A Dimopoulos, Thierry Facon, Saad Z Usmani, Maria-Victoria Mateos, et al. Evaluation of daratumumab for the treatment of multiple myeloma in patients with high-risk cytogenetic factors: a systematic review and meta-analysis. JAMA oncology, 6(11):1759–1765, 2020.
- [12] Richard M Goldberg. N9741: a phase iii study comparing irinotecan to oxaliplatin-containing regimens in advanced colorectal cancer. Clinical colorectal cancer, 2(2):81, 2002.

- [13] Tian Gu, Jeremy Michael George Taylor, and Bhramar Mukherjee. A synthetic data integration framework to leverage external summary-level information from heterogeneous populations. Biometrics, 79(4):3831–3845, 2023.
- [14] Patricia Guyot, AE Ades, Mario JNM Ouwers, and Nicky J Welton. Enhanced secondary analysis of survival data: reconstructing the data from published kaplan-meier survival curves. BMC medical research methodology, 12:1–13, 2012.
- [15] Waldemar Hahn, Jan-Niklas Eckardt, Christoph Röllig, Martin Sedlmayr, Jan Moritz Middeke, and Markus Wolfien. Generating reliable synthetic clinical trial data: The role of hyperparameter optimization and domain constraints. arXiv preprint arXiv:2505.05019, 2025.
- [16] Bruce Hajek. Cooling schedules for optimal annealing. Mathematics of operations research, 13(2):311–329, 1988.
- [17] Feifang Hu, Yanqing Hu, Zhenjun Ma, and William F Rosenberger. Adaptive randomization for balancing over covariates. Wiley Interdisciplinary Reviews: Computational Statistics, 6(4):288–303, 2014.
- [18] Yanqing Hu and Feifang Hu. Asymptotic properties of covariate-adaptive randomization. The Annals of Statistics, 40(3):1794 – 1815, 2012.
- [19] Jared L Katzman, Uri Shaham, Alexander Cloninger, Jonathan Bates, Tingting Jiang, and Yuval Kluger. Deepsurv: personalized treatment recommender system using a cox proportional hazards deep neural network. BMC medical research methodology, 18(1):24, 2018.

- [20] S. Kirkpatrick, C. D. Gelatt, and M. P. Vecchi. Optimization by simulated annealing. Science, 220(4598):671–680, 1983.
- [21] J Jack Lee and Chen-Hsing Tseng. Uniform power method for sample size calculation in historical control studies with binary response. Controlled Clinical Trials, 22(4):390–400, 2001.
- [22] Yunzhi Lin, Ming Zhu, and Zheng Su. The pursuit of balance: an overview of covariate-adaptive randomization techniques in clinical trials. Contemporary clinical trials, 45:21–25, 2015.
- [23] Na Liu, Yanhong Zhou, and J Jack Lee. Ipdfromkm: reconstruct individual patient data from published kaplan-meier survival curves. BMC medical research methodology, 21(1):111, 2021.
- [24] Yang Liu and Feifang Hu. The impacts of unobserved covariates on covariate-adaptive randomized experiments. The Annals of Statistics, 51(5):1895–1920, 2023.
- [25] Wei Ma, Feifang Hu, and Lixin Zhang. Testing hypotheses of covariate-adaptive randomized clinical trials. Journal of the American Statistical Association, 110(510):669–680, 2015.
- [26] Wei Ma, Ping Li, Li-Xin Zhang, and Feifang Hu. A new and unified family of covariate adaptive randomization procedures and their properties. Journal of the American Statistical Association, 119(545):151–162, 2024.
- [27] María-Victoria Mateos, Meletios A Dimopoulos, Michele Cavo, Kenshi Suzuki, Andrzej Jakubowiak, Stefan Knop, Chantal Doyen, Paulo Lucio, Zsolt Nagy, Polina Ka-

- plan, et al. Daratumumab plus bortezomib, melphalan, and prednisone for untreated myeloma. New England Journal of Medicine, 378(6):518–528, 2018.
- [28] Philippe Moreau, Maria-Victoria Mateos, James R Berenson, Katja Weisel, Antonio Lazzaro, Kevin Song, Meletios A Dimopoulos, Mei Huang, Anita Zahlten-Kumeli, and A Keith Stewart. Once weekly versus twice weekly carfilzomib dosing in patients with relapsed and refractory multiple myeloma (arrow): interim analysis results of a randomised, phase 3 study. The Lancet Oncology, 19(7):953–964, 2018.
- [29] Alexander Norcliffe, Bogdan Cebere, Fergus Imrie, Pietro Lio, and Mihaela van der Schaar. Survivalgan: Generating time-to-event data for survival analysis. In International Conference on Artificial Intelligence and Statistics, pages 10279–10304. PMLR, 2023.
- [30] Antonio Palumbo, Asher Chanan-Khan, Katja Weisel, Ajay K Nooka, Tamas Masszi, Meral Beksac, Ivan Spicka, Vania Hungria, Markus Munder, Maria V Mateos, et al. Daratumumab, bortezomib, and dexamethasone for multiple myeloma. New England Journal of Medicine, 375(8):754–766, 2016.
- [31] Tra My Pham, James R Carpenter, Tim P Morris, Angela M Wood, and Irene Petersen. Population-calibrated multiple imputation for a binary/categorical covariate in categorical regression models. Statistics in medicine, 38(5):792–808, 2019.
- [32] Stuart J Pocock and Richard Simon. Sequential treatment assignment with balancing for prognostic factors in the controlled clinical trial. Biometrics, pages 103–115, 1975.
- [33] Zexin Ren, Zixuan Zhao, Qian Shi, Andrew Cowan, Will Ma, and En Xie. Leveraging ai for validating the association between minimal residual disease (mrd) and survival

- outcomes in multiple myeloma. Journal of Clinical Oncology, 43(16_suppl):7547–7547, 2025. PMID:.
- [34] Richard D Riley, Paul C Lambert, Jan A Staessen, Jiguang Wang, Francois Gueyffier, Lutgarde Thijs, and Florent Bouctou. Meta-analysis of continuous outcomes combining individual patient data and aggregate data. Statistics in medicine, 27(11):1870–1893, 2008.
- [35] William F Rosenberger, Oleksandr Sverdlov, and Feifang Hu. Adaptive randomization for clinical trials. Journal of biopharmaceutical statistics, 22(4):719–736, 2012.
- [36] Galen H Sasaki and Bruce Hajek. The time complexity of maximum matching by simulated annealing. Journal of the ACM (JACM), 35(2):387–403, 1988.
- [37] Martin Schumacher, G Bastert, H Bojar, K Hübner, M Olschewski, W Sauerbrei, C Schmoor, C Beyerle, RL Neumann, and HF Rauschecker. Randomized 2 x 2 trial evaluating hormonal treatment and the duration of chemotherapy in node-positive breast cancer patients. german breast cancer study group. Journal of Clinical Oncology, 12(10):2086–2093, 1994.
- [38] Michael Seo, Ian R White, Toshi A Furukawa, Hissei Imai, Marco Valgimigli, Matthias Egger, Marcel Zwahlen, and Orestis Efthimiou. Comparing methods for estimating patient-specific treatment effects in individual patient data meta-analysis. Statistics in medicine, 40(6):1553–1573, 2021.
- [39] Kristian Thorlund, Louis Dron, Jay JH Park, and Edward J Mills. Synthetic and external controls in clinical trials—a primer for researchers. Clinical epidemiology, pages 457–467, 2020.

- [40] John Wilder Tukey. Exploratory data analysis. Reading/Addison-Wesley, 1977.
- [41] U.S. Food and Drug Administration. Considerations for the design and conduct of externally controlled trials for drug and biological products. Guidance for industry, U.S. Department of Health and Human Services, Food and Drug Administration, 2023.
- [42] Saad Z Usmani, Hang Quach, Maria-Victoria Mateos, Ola Landgren, Xavier Leleu, David Siegel, Katja Weisel, Maria Gavriatopoulou, Albert Oriol, Neil Rabin, et al. Carfilzomib, dexamethasone, and daratumumab versus carfilzomib and dexamethasone for patients with relapsed or refractory multiple myeloma (candor): updated outcomes from a randomised, multicentre, open-label, phase 3 study. The Lancet Oncology, 23(1):65–76, 2022.
- [43] Ting Ye and Jun Shao. Robust tests for treatment effect in survival analysis under covariate-adaptive randomization. Journal of the Royal Statistical Society Series B: Statistical Methodology, 82(5):1301–1323, 2020.
- [44] Song Zhang, Jing Cao, and Chul Ahn. Calculating sample size in trials using historical controls. Clinical Trials, 7(4):343–353, 2010.
- [45] Yao Zhao, Haoyue Sun, Yantian Ding, and Yanxun Xu. Km-gpt: An automated pipeline for reconstructing individual patient data from kaplan–meier plots. 2025.
- [46] Yujie Zhao, Bo Yang, J Jack Lee, Li Wang, and Ying Yuan. Bayesian optimal phase ii design for randomized clinical trials. Statistics in Biopharmaceutical Research, 14(4):423–432, 2022.
- [47] Weijie Zheng, Mingfeng Li, Renzhong Deng, and Benjamin Doerr. How to use the

metropolis algorithm for multi-objective optimization? In Proceedings of the Genetic and Evolutionary Computation Conference Companion, pages 71–72, 2024.

- [48] Hong Zhu, Song Zhang, and Chul Ahn. Sample size considerations for historical control studies with survival outcomes. Journal of biopharmaceutical statistics, 26(4):657–671, 2016.